LIMNOLOGY
and
OCEANOGRAPHY

ASLO

Limnol. Oceanogr. 00, 2018, 00–00

doi: 10.1002/lno.10798

CO_2 limited conditions favor cyanobacteria in a hypereutrophic lake: An empirical and theoretical stable isotope study

Bryce R. Van Dam,[1]* **Craig Tobias**,[2] **Andreas Holbach**,[3] **Hans W. Paerl**,[1] **Guangwei Zhu**[4]

[1]Institute of Marine Sciences, University of North Carolina at Chapel Hill, Morehead City, North Carolina
[2]Department of Marine Sciences, University of Connecticut, Groton, Connecticut
[3]Institute of Applied Geosciences, Karlsruhe Institute of Technology, Karlsruhe, Germany
[4]State Key Laboratory of Lake Science and Environment, Nanjing Institute of Geography & Limnology, Chinese Academy of Sciences, Nanjing, China

Abstract

Harmful algal blooms (HABs) are a global problem, exacerbated by rising temperatures, cultural eutrophication, urbanization, and agricultural development. During these HABs, phytoplankton consumption of CO_2 may result in conditions of C limitation, where algal taxa best adapted for these conditions will be at a competitive advantage. Many cyanobacteria are capable of alleviating CO_2 limitation by a variety of strategies, including the active assimilation of HCO_3^-. In this study, we utilized a high-resolution, month-long time series of stable C isotopes and high-performance liquid chromatograph-based algal taxonomy in the hypereutrophic Lake Taihu, China, to investigate whether cyanobacteria are indeed advantaged by CO_2 limiting conditions. We employed a model of phytoplankton C acquisition to support the inferences derived from direct measurements. Diurnal cycles of production and respiration caused $\delta^{13}C_{DIC}$ to vary between −4‰ and −9‰, while $\delta^{13}C_{POC}$ varied between −29.6‰ and −19.6‰. Measured and modeled phytoplankton fractionation of DIC were positively correlated with pCO_2 and negatively correlated with cyanobacterial abundance, suggesting that CO_2 limitation preferentially favored increased cyanobacterial biomass, relative to other taxa. We propose that the ability of many cyanobacteria to access otherwise limiting pools of inorganic C is intrinsically linked with their capacity to cope with CO_2 limiting conditions, and may be a key factor in their dominance during HABs.

Harmful algal blooms (HABs) have become increasingly frequent worldwide, particularly in regions experiencing rapid population growth and subsequent cultural eutrophication (Anderson et al. 2002; Paerl and Huisman 2008, 2009; Lu et al. 2010; Xu et al. 2010). In eutrophic lakes, HABs are often dominated by cyanobacteria (CyanoHABs), some producing toxic metabolites, inducing hypoxia, causing fish kills, and leading to unsightly, odoriferous surface scums (Wu et al. 2006; Qin et al. 2010; Otten et al. 2012). CyanoHABs have been recognized as a serious environmental issue in Europe for centuries, and in North America since WWII. Blooms in rapidly developing countries, especially China, are increasingly problematic and pervasive (Liu et al. 2011; Paerl et al. 2014, 2015; Shi et al. 2015). While the negative water quality impacts of CyanoHABs have been the subject of concern, the effect of HABs on the biogeochemical cycling of carbon (C) has received less attention. Cyanobacteria have a relative advantage in their ability to use bicarbonate (HCO_3^-) and carbonate (CO_3^{2-}) in addition to CO_2, allowing them to access additional inorganic carbon pools when CO_2 becomes depleted during blooms (Miller et al. 1990; Price et al. 2008). As cyanobacteria often constitute a disproportionately large fraction of total biomass in eutrophic lakes, their activity may be a significant force in shaping lake C cycles. Future increases in temperature and cultural eutrophication are expected to increase the frequency and magnitude of CyanoHABs (McQueen and Lean 1987; Paerl and Huisman 2008), and these same factors may alter the global emission of greenhouse gasses from lakes (Tranvik et al. 2009; Pacheco et al. 2014).

As photoautotrophs draw down the partial pressure of CO_2 (pCO_2) during blooms, pH increases, which causes the carbonate equilibrium to shift from a speciation dominated by CO_2 toward one dominated by bicarbonate (HCO_3^-) or carbonate (CO_3^{2-}). Because CO_2 is the favored substrate for

*Correspondence: bvandam@live.unc.edu

Additional Supporting Information may be found in the online version of this article.

C_3 photosynthesis, this elevated pH may be associated with inorganic carbon limitation (Verspagen et al. 2014). Physiological adaptations to this CO_2 limitation are not uniform across phytoplankton taxa (Elzenga et al. 2000), and it has been suggested that cyanobacteria are best suited for these conditions (Matsuda and Colman 1995; Shapiro 1997). There is ample evidence cyanobacteria and other phytoplankton groups (Tortell 2000; Reinfelder 2011) use carbon-concentrating mechanisms (CCMs) to alleviate CO_2 limitation (Aizawa and Miyachi 1986; Price 2011; Mangan et al. 2016; Sandrini et al. 2016), allowing them to thrive across a wide range of CO_2 concentrations (Paerl 1983; Morales-Williams et al. 2017). The CCMs of cyanobacteria are different from other taxa in that they function at very high carbon concentrating factors (external C : internal C), and at very low specificity factors of RuBisCo (Tortell 2000). These specific CCMs contribute to the relatively high efficiency of nitrogen use in cyanobacteria during photosynthesis (Price et al. 2008). Furthermore, bioassays indicate that picocyanobacteria outcompete eukaryotic phytoplankton in low CO_2 treatments (Li et al. 2016), and that microcystin concentrations increase in elevated CO_2 treatments (Yu et al. 2014). The effect of increasing atmospheric CO_2 levels on HABs in eutrophic lakes remains uncertain, particularly when assessed over diel or shorter time scales, which may be significant in highly productive lakes. It is still unclear how CO_2 limitation may affect phytoplankton taxonomic composition and C biogeochemistry when assessed over daily to weekly time scales, in the absence of experimental pCO_2 manipulations.

Lake C cycling is complex, involving exchanges with the atmosphere, sediments, and tributaries, as well as biotic and abiotic transformations of organic and inorganic forms of C. These biogeochemical transformations and exchanges, among others, cause the concentration and stable isotopic signature of particulate organic C ($\delta^{13}C_{POC}$) to vary over time. Changes in concentrations and isotopic compositon of particulate organic carbon (POC) have been used as a diagnostic tool to better understand; food web structures (de Kluijver et al. 2012; Smyntek et al. 2012), interactions between lakes and their watersheds (Maberly et al. 2013; Toming et al. 2013), and the effects of a changing climate (Marotta et al. 2014; Verspagen et al. 2014). Despite the complexity of C cycling, a few factors are primarily responsible for the majority of the $\delta^{13}C_{POC}$ variability in eutrophic, subtropical lakes. Thus, the interactions between phytoplankton and the inorganic C used for photosynthesis can be modeled with relatively few measured pools and assumptions (Rau et al. 1996, 1997). Specifically, positive relationships between bloom-driven pH changes and $\delta^{13}C_{POC}$ have been observed in lakes over time scales ranging from weekly (Gu et al. 2006), to annual (Gu et al. 2011), to decadal (Smyntek et al. 2012). The use of stable isotopes for investigating C cycling in lakes is made challenging by the fact that the isotopic signature of primary producers is influenced by multiple factors; (1) their growth rate, (2) concentrations and distributions of inorganic C species, (3) variable isotopic signatures of those species, (4) the kinetic isotope fractionations of relavent reactions, and (5) diffusional constraints on those enzymatic fractionations. Nevertheless, isotope-based models provide some mechanistic foundation to complement interpretations of observed changes or correlations measured in situ.

In this study, we measure stable isotopes of DIC and POC, along with proxies of algal taxonomy over diel to weekly time scales in the hypereutrophic Lake Taihu, China. This lake serves as an example of possible future conditions for other eutrophying lakes, globally. Specifically, we use these tools to investigate whether cyanobacteria, dominant taxa during summer blooms in Lake Taihu, gain an advantage under conditions of C limitation. This C limitation should be manifested isotopically as an enrichment in ^{13}C of their biomass, relative to the ^{13}C of their inorganic C source (i.e., decreased fractionation factor of RuBisCO under C-limiting conditions). We hypothesize that C limitation promotes the dominance of HAB-forming cyanobacteria in the water column below the surface scum, and test this hypothesis by comparing measured changes in phytoplankton community composition and pCO_2 with an isotope model simulation.

Methods

Study site

Lake Taihu, China's third largest freshwater lake (area of 2338 km^2), is situated along the lower reaches of the Yangtze River floodplain in the country's eastern Jiangsu province, approximately 100 km west of Shanghai (Fig. 1). This shallow ($\sim$ 2 m) hypereutrophic lake is polymictic, but regularly experiences temporary thermal stratification during warm periods. At least 40 million people inhabit its heavily urbanized 36,500 km^2 watershed, and $\sim$ 10 million people use the lake as a drinking water source (Qin et al. 2010). At the same time, Taihu experiences the demands of agricultural and industrial development in China's rapidly growing economy. Accelerating development has driven cultural eutrophication of the lake, symptomized by toxic CyanoHABs (Qin et al. 2010; Paerl et al. 2011).

Field measurements

Grab samples for all analyses were collected three times a day on a Dawn-Noon-Dusk schedule for a total of 26 d between 20 June 2016 and 18 July 2016. Samples were collected from the end of a $\sim$ 100 m long pier at the Taihu Laboratory for Lake Ecosystem Research (TLLER, Fig. 1). A plastic bucket, triple rinsed with site water, was used to collect site water from $\sim$ 10 cm below the surface, which was then homogenized and subsampled twice as pseudoreplicates. When floating scum was present on the water

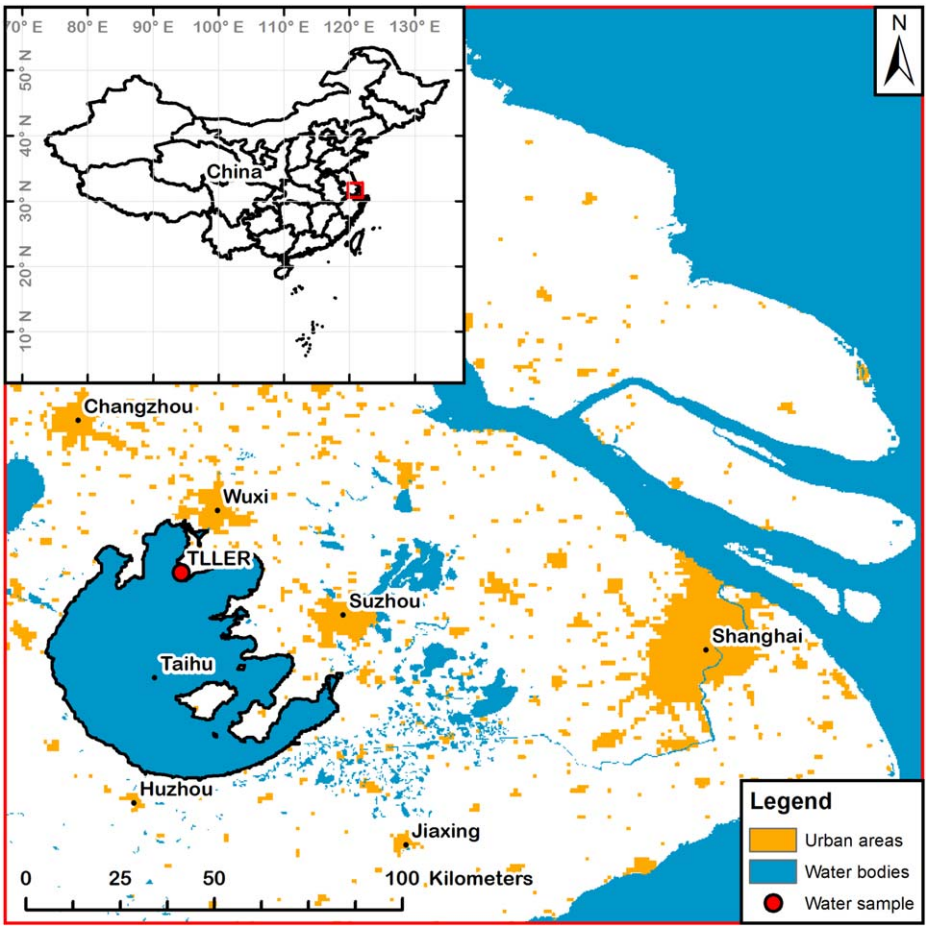

Fig. 1. Site map showing the location of Lake Taihu and the Taihu Laboratory for Lake Ecosystem Research (TLLER) in Jiangsu Province, China. Map produced using the Globcover database published by the European Space Agency (http://due.esrin.esa.int/page_globcover.php). [Color figure can be viewed at wileyonlinelibrary.com]

surface, it was also collected. A multiparameter sonde (Yellow Springs, Yellow Springs, Ohio) and meteorological station deployed at the end of the pier provided background environmental and physicochemical data. Major soluble nutrients [total dissolved nitrogen (TDN), total dissolved phosphorus (TDP), phosphate (PO_4), ammonium (NH_4)] were measured in surface-water samples collected near the beginning, middle, and end of the study using analytical methods described in Paerl et al. (2015).

Dissolved gasses

Before additional samples were taken from the bucket, two 60 mL syringes were filled to 30 mL with site water, to which 30 mL of CO_2-free air (ambient air passed through a soda lime scrubber) was immediately added. These syringes were vigorously shaken in the shade for 60 s, after which the headspace was injected into pre-evacuated 10 mL Exetainers (Labco Limited, UK) with double wadded septa caps. A combination of these vials and septa can limit sample loss to insignificant amounts for at least 3 months (Eby et al. 2015). Headspace and ambient samples were analyzed for CO_2 and CH_4 by GC at the Nanjing Institute of Geography and Limnology (NIGLAS), Chinese Academy of Sciences. In situ partial pressures were calculated from headspace concentrations using Henry's Law, along with a temperature dependent solubility according to Wanninkhof (1992). Ambient air passed through the soda lime scrubber was found to contain a small amount of CO_2. This small residual amount of CO_2 was accounted for in the previous calculations. DIC samples were filtered in the field through pre-combusted 25 mm GF/F filters into containers with no headspace. These samples were stored in a refrigerator until DIC could be measured with a Shimadzu TOC analyzer in inorganic carbon mode (TOC-5000A). An in situ membrane based CO_2 detector (Turner Designs C-sense) deployed $\sim$ 0.5 m below the surface and serviced every 3–5 d, provided data to fill in when headspace equilibration CO_2 determinations did not repeat or were missing. Membrane-based sensors such as the C-sense

operate reasonably well for long term deployments when they are serviced regularly (Abril et al. 2015; Yoon et al. 2016).

Phytoplankton photopigments

Water samples were vacuum-filtered on 25 mm GF/F filters, blotted dry, folded, frozen, and transported (frozen) to The University of North Carolina at Chapel Hill, Institute of Marine Sciences for analysis. Filters were extracted in 100% acetone, sonicated, and stored at 0°C for approximately 24 h. Extracts (200 mL) were then injected by an autosampler into a Shimadzu SIL-20AC HT high-performance liquid chromatograph (HPLC) equipped with a SPD M10Avp photodiode array detector, following procedures described by Van Heukelem et al. (1994) and Pinckney et al. (2001). In addition to chlorophyll *a* (Chl *a*), phytoplankton class-specific diagnostic photopigments were quantified using HPLC, including: fucoxanthin (diatoms), myxoxanthophyll, zeaxanthin, and echinenone (cyanobacteria), alloxanthin (cryptophytes), and chlorophyll *b* and lutein (chlorophytes). Pigments were identified according to their absorption spectra, using commercial pigment standards (DHI, Denmark). Contributions of the dominant four algal classes (chlorophytes, cryptophytes, cyanobacteria, and diatoms) to total phytoplankton community in response to nutrient manipulations were calculated using Chemtax (Mackey et al. 1996). The input pigment ratio matrix for the four classes was adapted from a study of lacustrine phytoplankton species (Schlüter et al. 2006; Paerl et al. 2014). Input pigment matricies of Mackey et al. (1996) and Lewitus et al. (2005) were used to test the sensitivity of Chemtax output to different algal class-specific pigment ratios.

Stable isotope analysis

POC and DIC were analyzed for ^{13}C composition. Water samples were vacuum-filtered on pre-combusted 25 mm GF/F filters, oven dried (60°C), frozen, and transported to the stable isotope facility at the University of Connecticut (UConn) Department of Marine Sciences for analysis of $\delta^{13}C_{POC}$ on a Thermo Delta V isotope ratio mass spectrometer coupled to an elemental analyzer (EA-IRMS). Surface scum samples were also analyzed for $\delta^{13}C$ as above, and all samples were acid-fumed prior to EA-IRMS analysis to remove any carbonates trapped on the filters or in the scum matrix. Duplicate filters were also treated identically and analyzed for POC and total nitrogen (TN), using a Costech ECS 4010 combustion analyzer. Water samples for $\delta^{13}C_{DIC}$ analysis were collected and filtered in the field with pre-combusted 25 mm GF/F filters into containers with no headspace, and kept in the shade until they could be processed in the lab (within an hour). Briefly, 30 mL of site water was filtered to remove any potential inorganic C precipitate (combusted 25 mm GF/F). Filtered water was then introduced to a pre-acidified (conc. HCl) 60 mL syringe, to which 30 mL of He was added. Syringes were vigorously shaken for at least 60 s, after which, the headspace was injected into evacuated 12 mL Exetainers. These samples, as well as field blanks, were stored in a refrigerator before being shipped to the stable isotope lab at UConn. The interpretation of $\delta^{13}C_{POC}$ trends is complicated by the fact that the $\delta^{13}C_{POC}$ at any given time is not simply representative of the source $\delta^{13}C_{DIC}$ and fractionation factor, but also represents the residual $^{13}C_{POC}$ that was fixed previously. To correct $\delta^{13}C_{POC}$ for any such residual pool effects, the $\delta^{13}C$ of biomass fixed ($\delta^{13}C_{fixed}$) was calculated for each time-step (t_{n-1} to t_n) using $\delta^{13}C_{POC}$ and POC concentrations, such that $\delta^{13}C_{fixed}$ represents the average $\delta^{13}C_{POC}$ fixed during each time-step.

$$\delta^{13}C_{fixed} = \frac{\left[\left(\delta^{13}C_{POC_{t_1}} * POC_{t_1}\right) + \left(\delta^{13}C_{POC_{t_1}} * POC_{t_{n-1}}\right)\right] * (POC_{t_1} - POC_{t_{n-1}})}{POC_{t_1}}$$

Two independent methods were then employed to estimate effective in situ isotope fractionation factors (ε_p) from direct measurements of $\delta^{13}C_{POC}$ and $\delta^{13}C_{DIC}$. First, the fractionation factor between inorganic C and recently fixed phytoplankton biomass ($\varepsilon_{p\text{-}POC}$) was calculated as $\delta^{13}C_{fixed} - \delta^{13}C_{DIC}$. Second, a Rayleigh distillation approach was used to quantify the photosynthetic fractionation factor ($\varepsilon_{p\text{-}DIC}$) using changes in the DIC pool, where $\varepsilon_{p\text{-}DIC}$ was calculated as the increase in $\delta^{13}C_{DIC}$ for a given change in the fraction of DIC consumed (Supporting Information Fig. S1). This Rayleigh distillation approach was only used for days when a complete record existed (morning, noon, and dusk measurements) where $\delta^{13}C_{DIC}$ increased with the fraction of DIC consumed ($n = 9$ d). $\varepsilon_{p\text{-}DIC}$ values computed for overnight time periods are not presented, but were generally $\sim 0‰$, in line with expected values for periods of no photosynthesis.

Modeling

Multiple factors affect the $\delta^{13}C$ of phytoplankton biomass ($\delta^{13}C_{phyto}$), including $\delta^{13}C_{DIC}$, CO_2 availability, intrinsic growth rates, and the biochemical pathway of C acquisition, which has some imperfect efficiency due to CO_2 leakage (Fig. 2). Because of the difficulty in isolating phytoplankton biomass from suspended organic matter, trends in $\delta^{13}C_{POC}$ are often assumed to be representative of $\delta^{13}C_{phyto}$, an appropriate assumption in Taihu, where nearly all of the

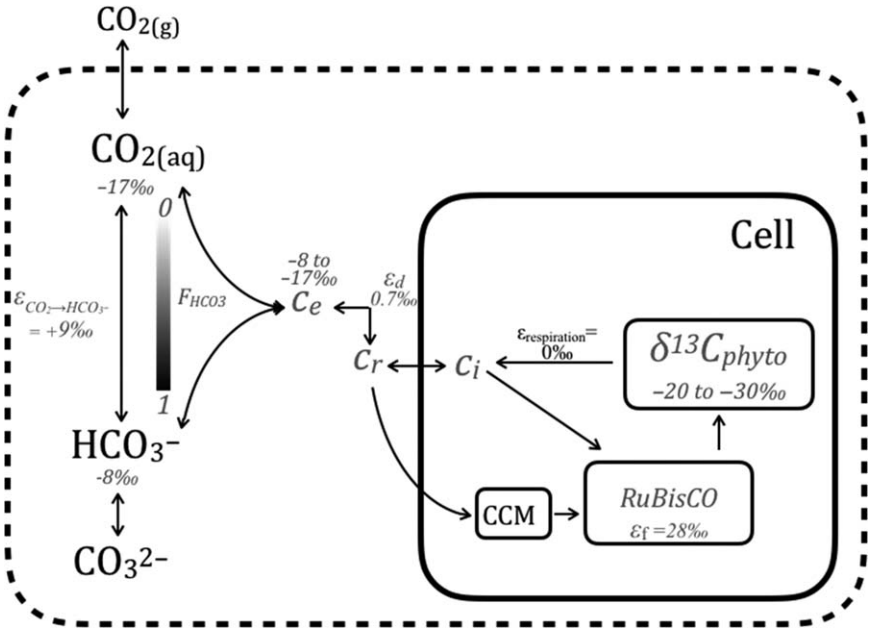

Fig. 2. Conceptual figure describing how ^{13}C was partitioned between cellular and environmental pools. Gray, italicized terms were modeled.

POC pool is composed of phytoplankton biomass. For DIC uptake by phytoplankton, the $\delta^{13}C$ and pool size of inorganic carbon being assimilated is not always the same as the bulk DIC pool. Photosynthetic fixation of intracellular CO_2 (c_i), leads to a reduction of c_i relative to extracellular CO_2 (c_e). This gradient between c_e : c_i drives diffusion of CO_2 across cell membranes; therefore, if the influence of CO_2 availability on phytoplankton is to be assessed, then c_i (which cannot be directly measured) is the variable of interest, rather than c_e. In this study, a model was used to directly calculate both ε_p and $\delta^{13}C_{phyto}$, both of which represent phytoplankton physiology more closely than does measured $\delta^{13}C_{POC}$, and by extension yield estimates of c_i. Collectively, these model outputs permit the assessment of the carbon limitation status of phytoplankton, and when combined with taxonomy and biomass, help to address the primary research question of the role of carbon limitation in maintaining cyanobacterial dominance during large blooms. A summary of model terms and their respective abbreviations are shown in Table 1.

The concentrations and $\delta^{13}C$ of organic and inorganic C pools were modeled using a system of linear and nonlinear equations. The model consisted of one POC pool (C_{phyto}), three DIC pools (c_e, c_r, and c_i), and three reactions that include both equilibrium and kinetic fractionation effects ($c_e \rightleftharpoons c_r$, $c_r \rightleftharpoons c_i$, $c_i \rightleftharpoons C_{phyto}$). The model was initialized with directly measured DIC and $\delta^{13}C_{DIC}$ (c_e pool), and the following unmeasured parameters that were derived from the literature: cell radius (r), enzymatic fractionation factor (ε_f), diffusion fractionation factor (ε_d), cell wall permeability (P), fraction of DIC assimilated as HCO_3^- (F_{HCO3}), ratio of light to dark hours ($L : D$), and growth rate (μ). Details of the model that was adapted for this study can be found in Rau et al. (1996, 1997), and are depicted in Fig. 2. More sophisticated models have been developed for idealized diatoms (Hopkinson 2014, 2016) and cyanobacteria (Eichner et al. 2015; Hinners et al. 2015), which allow for multiple c_i compartments. A model with such detail may be informative when paired with empirical data from a manipulative chemostat or mesocosm experiment, but would be challenging to assess against bulk environmental data as were collected in this study. Parameters informing the model, along with values used as base conditions, are shown in Table 2.

The model was parameterized in a stepwise manner, starting with the aqueous $\delta^{13}C_{CO2}$ boundary condition, which diffuses toward the internal CO_2 pool ($\delta^{13}C_{ci}$), allowing the ratio of internal to external CO_2 (c_i/c_e) to be used as a scaling factor for the calculation of $\delta^{13}C_{phyto}$ values. First, the ambient aqueous CO_2 concentration (c_e) was calculated using the carbonic acid dissociation constants of Cai and Wang (1998), and an assumed pCO_2 (range listed in Table 2) and pH. Next, a temperature-dependent fractionation factor equilibrium was used to determine the isotopic signature of CO2 ($\delta^{13}C_{CO2}$) from measured $\delta^{13}C_{DIC}$ (Mook et al. 1974):

$$\delta^{13}C_{CO2} = \delta^{13}C_{DIC} + 23.6 - \left(\frac{9701.5}{T_K}\right) \quad (1)$$

Because measured $\delta^{13}C_{DIC}$ was found to correlate with pH in Taihu, we treated it as a boundary condition and set $\delta^{13}C_{DIC}$ as a function of pH such that $\delta^{13}C_{DIC} = (0.73 * pH) - 13.8$

Table 1. Definitions of commonly used terms derived from measurements and modeling.

Term		Description
$\delta^{13}C_{DIC}$	Measured	Stable isotopic composition of DIC
$\delta^{13}C_{POC}$	Measured	Stable isotopic composition of POC
$\delta^{13}C_{fixed}$	Calculated	Stable isotopic composition of C fixed since last time point
$\varepsilon_{p\text{-}POC}$	Calculated	Fractionation factor calculated from $\delta^{13}C_{fixed}$ and $\delta^{13}C_{DIC}$
$\varepsilon_{p\text{-}DIC}$	Calculated	Fractionation factor calculated by Rayeigh distillation
$\delta^{13}C_{phyto}$	Modeled	Stable isotopic composition of phytoplankton biomass
c_e, $\delta^{13}C_{ce}$	Modeled	DIC used by phytoplankton, and its $\delta^{13}C$ (set by F_{HCO3}; Eq. 2)
c_r, $\delta^{13}C_{cr}$	Modeled	DIC at the cell surface, and its $\delta^{13}C$
c_i, $\delta^{13}C_{ci}$	Modeled	DIC inside the cell, and its $\delta^{13}C$
$\varepsilon_{p\text{-}model}$	Modeled	Total photosynthetic fractionation factor

Table 2. Model parameters, base values, and ranges over which values were adjusted to optimize model fit.

Description	Model term	Units	Base value	Min	Max
Intracellular enzymatic fractionation factor	ε_f	‰	18	10	20
Diffusive fractionation factor	ε_d	‰	0.7	Constant	
Intracellular $[CO_2]_{aq}$	c_i	mM	3.9	Varies with T, r, and μ	
Ambient $[CO_2]_{aq}$	c_e	mM	6.4	1.6	95.0
Cell radius	r	μm	100	2.5	200
Partial pressure CO_2	pCO_2	μatm	400	100	2000
Temperature	T	°C	27	22	32
Cell wall permeability to CO_2	P	m s^{-1}	5×10^{-5}	1×10^{-5}	50×10^{-5}
Fraction of DIC assimilated as HCO_3^-	F_{HCO3}	Ratio	0.5	0	1
Ratio of light to dark hours	$L{:}D$	Ratio	0.6	0.2	0.6
Instantaneous growth rate	μ	d^{-1}	3	0.4	4

($r^2 = 0.16$, $p < 0.005$). Similarly, modeled pH was set to vary with pCO_2 (μatm) according to the empirically determined log-linear relationship: $pH = -0.52 * \log(pCO_2) + 11.6$ ($r^2 = 0.81$, $p < 0.0001$). As some phytoplankton in Taihu are capable of assimilating HCO_3^- and these two inorganic carbon pools have different $\delta^{13}C$ values (approximately −7.5‰ and −16‰ for HCO_3^- and CO_2, respectively), the net inorganic C used for photosynthesis ($\delta^{13}C_{ce}$) was allowed to vary with the fraction of DIC assimilated as HCO_3^- (F_{HCO3}):

$$\delta^{13}C_{ce} = \left(F_{HCO3} \times \delta^{13}C_{DIC}\right) + \left[(1 - F_{HCO3}) \times \delta^{13}C_{CO2}\right] \quad (2)$$

Given the high pH observed in Taihu during the study period, virtually all DIC was present as HCO_3^-, allowing $\delta^{13}C_{DIC}$ to be used in place of $\delta^{13}C_{HCO3}$ in Eq. 2. Next, with the distribution of inorganic carbon outside the cell parameterized, CO_2 diffusion toward and into the cell was parameterized according to the following Arrhenius-style equation:

$$D_T = 5.019 \times 10^{-6} \times e^{-\left(E_d / R \times T_K\right)} \quad (3)$$

where E_d, the activation energy, is 19,510 J mol^{-1}, R is the ideal gas constant (8.3143 J K^{-1} mol^{-1}, and T_K is temperature (K). D_T, is then used to calculate the CO_2 concentration at the cell surface (c_r), assuming the dimensions of a single, idealized, spherical cell. The concentration of CO_2 inside the cell (c_i) was then set by the diffusive flux of CO_2 across the cell membrane (Q_s), relative to the membrane permeability (P), for an assumed spherical cell:

$$c_i = c_r - \frac{Q_s}{P} \quad (4)$$

Finally, the isotopic composition of phytoplankton biomass ($\delta^{13}C_{phyto}$) was calculated using the CO_2 concentration gradient (c_i/c_e) as a scaling factor:

$$\delta^{13}C_{phyto} = \delta^{13}C_{ce} - \varepsilon_d - (\varepsilon_f - \varepsilon_d)\frac{c_i}{c_e} \quad (5)$$

Variations in $\delta^{13}C_{phyto}$ were assessed in the context of c_e, as an indicator of carbon limitation. The model was initialized with isotope fractionation factors for diffusion (ε_d) and enzyme (RuBisCO) kinetics (ε_f), set at 0.7‰ (O'Leary 1984) and 18‰ (Popp et al. 1998), respectively. The total fractionation factor

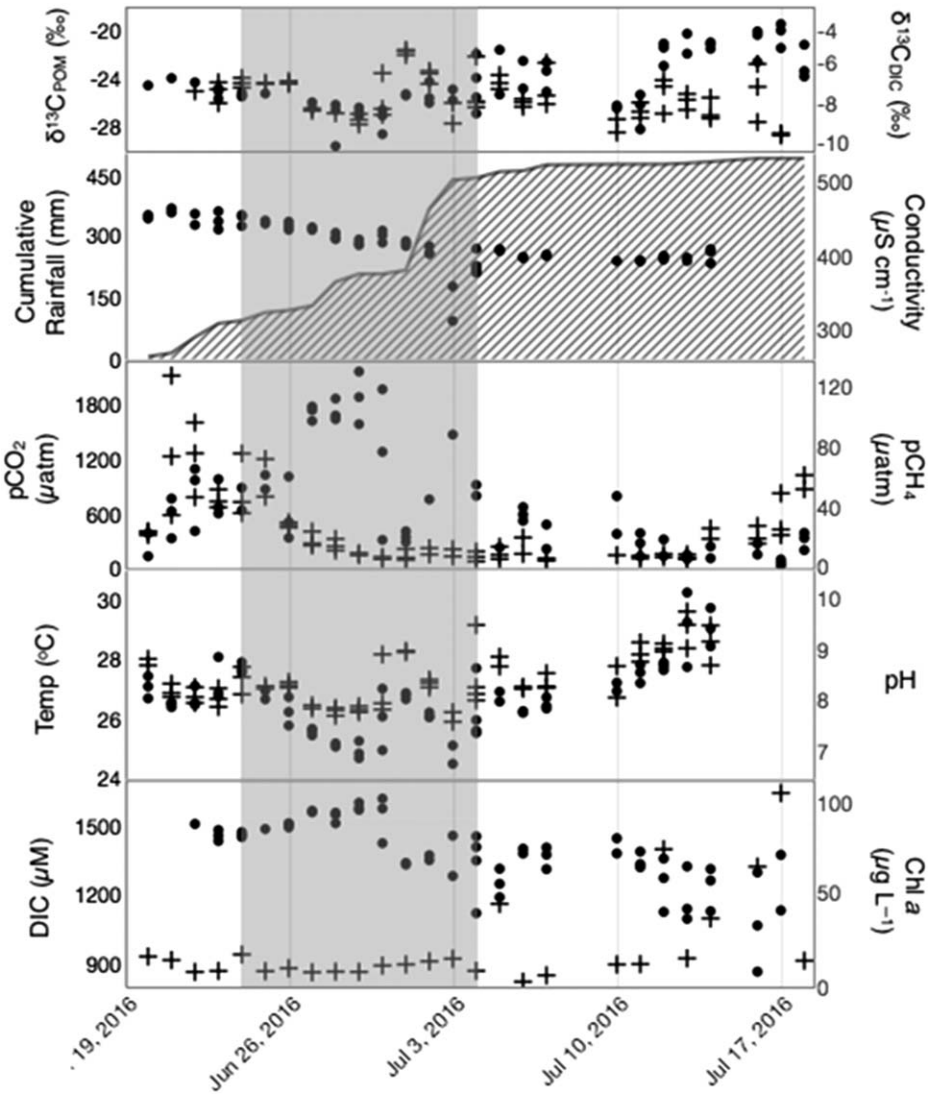

Fig. 3. Time-series plot of physical and chemical properties. Plus symbols correspond with the right axis, while filled black points correspond to the left axis. The gray area indicates the approximate duration of the monsoon period.

for net inorganic carbon fixation, $\varepsilon_{\text{p-model}}$, was calculated with the following equation, assuming a cell radius (r) of a single, spherical cell:

$$\varepsilon_{\text{p-model}} = \varepsilon_{\text{f}} + \frac{-\left[(\varepsilon_{\text{f}} - \varepsilon_{\text{d}}) \times Q_{\text{s}} \times \left(\frac{r}{D_{\text{T}}} + \frac{1}{P}\right)\right]}{c_{\text{e}}} \quad (6)$$

Equations 3–6 are derived from Rau et al. (1996).

Finally, the sensitivity of modeled $\delta^{13}C_{\text{phyto}}$ to each parameter listed in Table 2 was tested by holding all values constant except the parameter of interest, which was allowed to vary over the indicated range. For example, to asses the sensitivity of modeled $\delta^{13}C_{\text{phyto}}$ to changes in temperature, all other variables were held constant, and the model was run for temperatures ranging from 22°C to 32°C. The absolute value (in ‰) of the range in $\delta^{13}C_{\text{phyto}}$ obtained when each parameter was allowed to vary over the indicated range was considered to be the model sensitivity to that parameter.

Results

Physicochemical setting

This time-series study began with ~ 4 d of fairly calm conditions, followed by ~ 2 weeks of monsoon-like rains (24 June–04 July), which eventually gave way to 12 d of hot and relatively dry weather (05 July–18 July). During a very active monsoon period, cumulative precipitation reached nearly 500 mm (Fig. 3), causing the level of the lake to increase by at least 50% (~ 1 m). This rainfall caused conductivity during this period to decrease from 450 μS cm^{-1} to < 400 μS

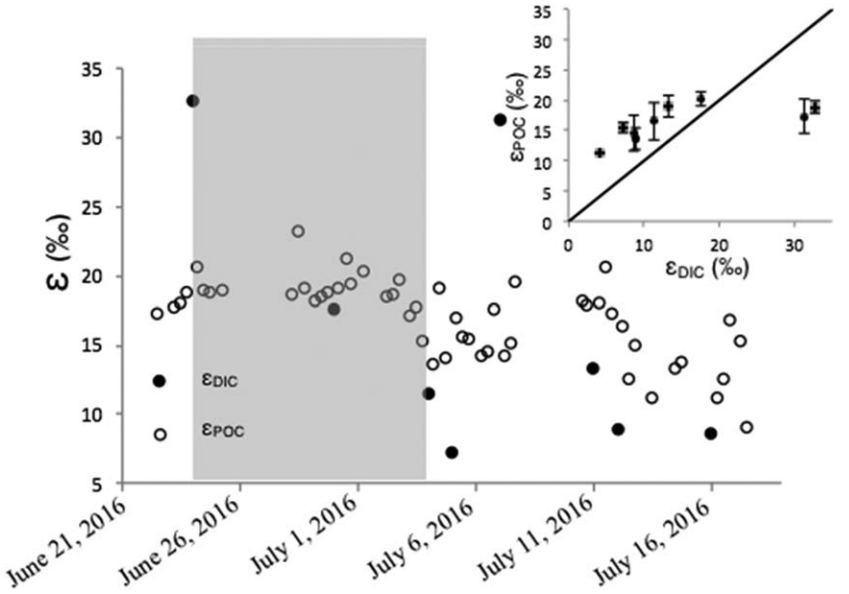

Fig. 4. Time series of ε_{DIC} and ε_{POC} (‰) and relationship between the two methods for calculating phytoplankton fractionation factors, falling approximately on the 1 : 1 line (inset). The shaded area indicates the approximate duration of the monsoon period.

cm^{-1}. A combination of external CO_2 inputs and net ecosystem heterotrophy drove pCO_2 to exceed 1000–2000 μatm during this period. This somewhat atypical weather pattern was also accompanied by high winds and river runoff, severely impacting water clarity.

Following the monsoon, water temperature increased by $\sim$ 5°C, and pCO_2 fell below equilibrium with the atmosphere, in association with a large phytoplankton bloom. Much of the bloom biomass was concentrated at the air–water interface as a surface scum. Despite being a fairly well buffered system (DIC consistently 1–1.5 mM), high growth rates drove pH to increase from <8 during the monsoon to >9.5 afterward. POC was highly variable, ranging from a low of 542 mg L^{-1} during the monsoon to 21,964 mg L^{-1} during peak bloom biomass, and was well correlated with Chl *a* ($R^2 = 0.97$), suggesting that the majority of OC present in the lake at any given time was algal in origin. It is important to note that these are POC concentrations for seston sampled $\sim$ 0.1 m below the surface, thus excluding any surface scum. When scum was present, vertically integrated POC was likely much greater than what is reported here. Average C : N ratio of POC was 6.1, and was fairly stable over the study period, ranging between 5.0 and 7.2. These low C : N ratios further suggest that the vast majority of material contributing to POC was of phytoplankton origin, and not terrestrial or macrophyte-derived. Dissolved nutrients (TDN, TDP, PO_4, NH_4) were high, and decreased steadily over the study period (TDN = 0.5–1.5 mg L^{-1}, TDP = 0.025–0.05 mg L^{-1}). The average molar ratio of Total Nitrogen : Total Phosphorus, including dissolved and particulate fractions, was 38, decreasing only slightly over the study period, suggesting that P may have been limiting. Average TDN : TDP was 59.4, but was more variable through time.

Algal taxonomy

According to Chemtax modeling of diagnostic photopigments, cyanobacteria and chlorophytes together were responsible for 73% (36% and 37%, respectively) of total Chl *a*, when averaged across the study period, similar to other recent studies (Paerl et al. 2014, 2015). During the monsoon, diatoms and chlorophytes roughly doubled in relative abundance, from 3.8% to 8.6% and $\sim$ 30.3% to 51.3%, respectively, while cyanobacteria reached a minimum of 20.0% (Fig. 5). Following the monsoon, the community became dominated by cyanobacteria, with this class reaching a high of 51.7% of total Chl *a*. The relative abundance of cyanobacteria was likely underestimated during these peak bloom periods because buoyant cell aggregations (common of *Microcystis* spp.) rose to the surface, and were thus not included in bulk water collection. Nevertheless, as previous studies in Taihu have shown, calm and hot conditions are commonly associated with cyanobacterial dominance (Paerl and Huisman 2008; Qin et al. 2010; Li et al. 2016).

Stable isotopes

Stable isotopes of POC and DIC were variable; initial $\delta^{13}C_{POC}$ values were approximately $-25‰$, fluctuated between $-29.6‰$ and $-22.0‰$ during the monsoon, then rose to a maximum of $-19.6‰$ upon the initiation of the bloom (Fig. 3). As has been documented previously, $\delta^{13}C_{POC}$ was negatively exponentially correlated with $[CO_2]_{(aq)}$ (Gu et al. 2006; Smyntek et al. 2012; Morales-Williams et al. 2017). In the present study, $\delta^{13}C_{POC}$ varied inversely with the logarithm of

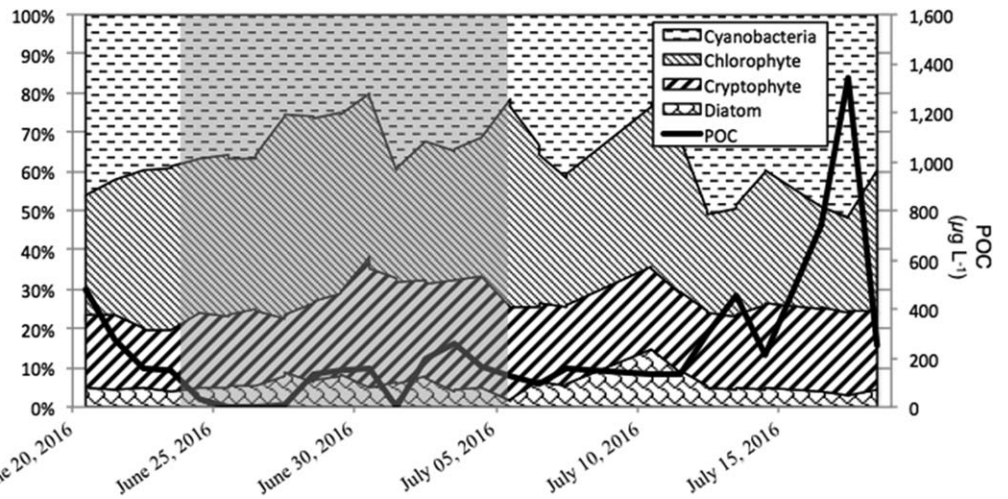

Fig. 5. Proportion of Chl *a* represented by major phytoplankton taxa, as a fraction of total Chl *a* and POC (μg L^{-1}). The shaded area indicates the approximate duration of the monsoon period.

$[CO_2]_{aq}$, such that $\delta^{13}C_{POC} = -1.1 * \ln([CO_2]_{(aq)}) - 22.3$ ($R^2 = 0.42$). $\delta^{13}C_{DIC}$ varied over a smaller range, between $-9.6‰$ and $-5.4‰$, with no clear trends over the entire study period. $\delta^{13}C_{Fixed}$ was significantly related to both temperature and pH ($p < 0.0001$), but no clear relationship between $\delta^{13}C_{DIC}$ and $\delta^{13}C_{POC}$ was found ($R^2 < 0.001$, p value > 0.93). The difference between $\delta^{13}C_{POC}$ and calculated $\delta^{13}C_{fixed}$ (derived from $\delta^{13}C_{POC}$ and POC) was generally small (average = 0.3‰), suggesting that the bulk POC was turning over rapidly enough such that $\delta^{13}C_{POC}$ was not significantly impacted by the antecedent $\delta^{13}C_{POC}$. $\varepsilon_{p\text{-}POC}$ is the in situ enrichment factor relating changes in either POC or DIC to changes in $\delta^{13}C$, and represents the net result of all processes affecting that pool. $\varepsilon_{p\text{-}POC}$ was variable but generally decreased over the study period, and was significantly positively correlated with pCO_2 (Fig. 4). With the exception of two outlier values, $\varepsilon_{p\text{-}DIC}$ and $\varepsilon_{p\text{-}POC}$ values were linearly related and followed the same trend over time, with $\varepsilon_{p\text{-}DIC}$ always less than $\varepsilon_{p\text{-}POC}$ (Fig. 4, inset).

This study used a model to estimate ε_p and $\delta^{13}C_{phyto}$, both of which represent phytoplankton physiology more precisely than bulk $\delta^{13}C_{POC}$. For example, measured $\delta^{13}C_{Fixed}$ was strongly correlated with DIC and pCO_2, but many other variables auto-correlate with DIC and pCO_2, including temperature and phytoplankton growth rate, both of which are likely to affect $\delta^{13}C_{phyto}$. Disentangling the relative importance of these various factors was a key goal of this modeling exercise. Figure 9a shows that the modeled $\delta^{13}C_{phyto}$ values were in general agreement with $\delta^{13}C_{Fixed}$, indicating that the model captured natural variations in $\delta^{13}C$ reasonably well. Both $\delta^{13}C_{phyto}$ and $\delta^{13}C_{Fixed}$ exhibited the same inverse and logarithmic relationship with pCO_2, which is consistent with previous observations of a strong dependence of $\delta^{13}C_{phyto}$ on ambient $[CO_2]_{aq}$ concentration (Rau et al. 1997; Gu et al. 2006; Lammers et al. 2017). However, the observed relationship between $\delta^{13}C_{Fixed}$ (and $\delta^{13}C_{phyto}$) and c_e cannot be directly attributed to changes in phytoplankton fractionation, because the pool of DIC utilized by phytoplankton is not isotopically constant, but instead varies with a variety of factors, including air–water exchange, pH, and lateral DIC inputs (Fig. 2). Furthermore, it is well documented that CO_2 leakage from the CCM will result in isotopic enrichment of the c_i pool, proporational to the $c_i : c_e$ gradient (Burkhardt et al. 1999; Eichner et al. 2015). The phytoplankton fractionation factor, ε_p, accounts for changes in the $\delta^{13}C$ of both the reactant (DIC) and product (POC), and is therefore a more appropriate term for gauging the magnitude of carbon limitation. $\varepsilon_{p\text{-}POC}$ was 17–22‰ before the monsoon, became more variable during the storms (15–23‰), then fell as low as 9‰ after the initiation of the bloom, when DIC/CO_2 were rapidly consumed (Fig. 4). These relatively low fractionation factors are consistent with previously measured values for cyanobacteria of 2.7–13.6‰ (Popp et al. 1998; Lammers et al. 2017), and are far below the maximum photosynthetic fractionation factor typical of carbon-replete conditions (~ 30‰, Keller and Morel 1999). That both $\varepsilon_{p\text{-}DIC}$ and $\varepsilon_{p\text{-}POC}$ decreased during the bloom period (Fig. 4) suggests that the phytoplankton community in Taihu experienced carbon limited conditions during these high-growth, low pCO_2 periods, as discussed in the following section.

Discussion

Drivers of cyanobacterial abundance

The relative contribution of cyanobacteria to total Chl *a* was variable over the study period, ranging from 20.0% to 51.7% (Fig. 5), associated with changes in temperature, light, CO_2, and nutrient availability. The consistently high N : P ratios suggest that phytoplankton were nutrient-limited with respect to P, although previous bioassays in lake Taihu have

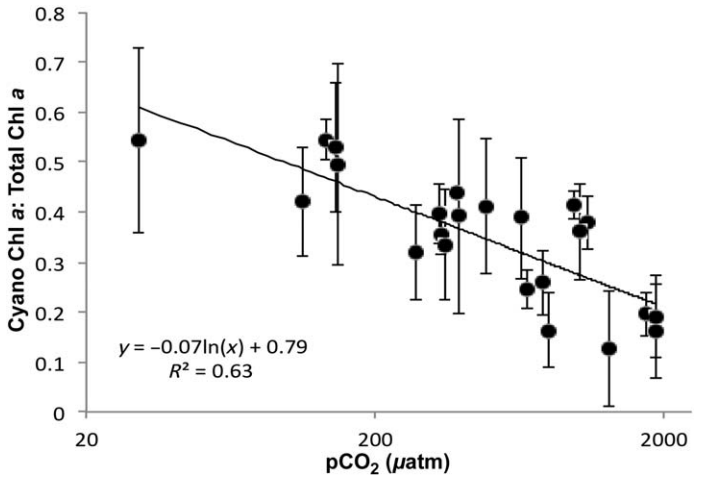

Fig. 6. Relationship between pCO_2 and the fraction of total Chl *a* represented by cyanobacteria. Individual data points and error bars represent the average and standard deviation of chemtax output using a range of previously published group-specific pigment ratios (Mackey et al. 1996; Lewitus et al. 2005; Schlüter et al. 2006; Paerl et al. 2014).

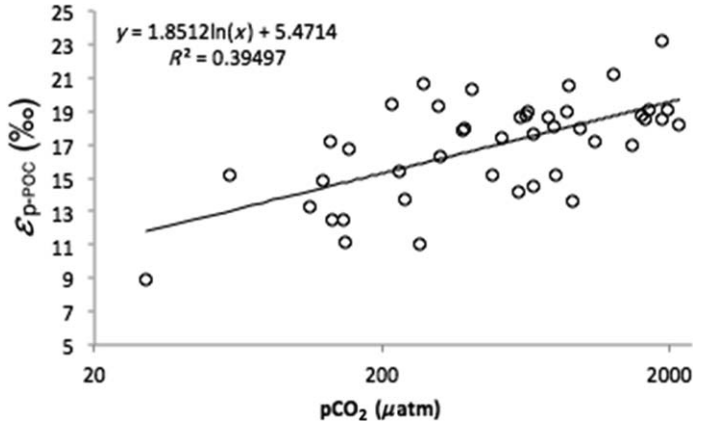

Fig. 7. Relationship between pCO_2 and $\varepsilon_{p\text{-}POC}$.

shown that intense recycling of N (as NH_4^+), along with the taxonomic dominance of non-N_2 fixing cyanobacteria, may promote N and P co-limitation (Paerl et al. 2014). Despite this P- or co-limitation, TDP was always relatively high, never falling below 0.02 mg L^{-1}. Figure 6 shows that the cyanobacterial contribution to Chl *a* was significantly negatively correlated with pCO_2 ($R^2 = 0.63$, $p < 0.001$), suggesting that CO_2 concentration, rather than N and P availability, was associated with the dominance of cyanobacteria. Low pCO_2 conditions were also accompanied by high temperature, a factor that may favor cyanobacteria through its effect on growth rate and thermal stratification (McQueen and Lean 1987; Paerl and Huisman 2008). Temperature and cyanobacterial Chl *a* were also positively correlated, but the relationship was weaker than that with pCO_2 ($R^2 = 0.32$). Hence, the relationship between cyanobacterial abundance and pCO_2 can be largely attributed to the role that C limitation played.

$\delta^{13}C_{POC}$

The observed post-monsoon decrease in $\varepsilon_{p\text{-}POC}$ coincided with a decrease in pCO_2 (and enrichment in $\delta^{13}C_{POC}$), and an increase in the abundance of cyanobacteria, relative to chlorophytes and cryptophytes (Figs. 4, 5). The cyanobacteria present in Taihu were buoyant, likely shading competing species (Paerl 1983). Additionally, cycanobacteria are effective at utilizing HCO_3^- when CO_2 availability is limited (Kaplan and Reinhold 1999; Badger and Spalding 2000; Sandrini et al. 2016). Furthermore, when these surface scums were present ($n = 13$), their $\delta^{13}C$ ($\delta^{13}C_{scum}$) was most often lighter than epilimnic $\delta^{13}C_{POC}$ ($n = 10$, 77%). This phenomenon was reported in Gu and Alexander (1997) and Xu et al. (2007), where the difference between $\delta^{13}C_{scum}$ and $\delta^{13}C_{POC}$ was significantly positively correlated with pH. We found no such relationship. We instead suggest that surface scums, rather than functioning as a separate biogeochemical pool, simply represent an aggregation of buoyant cyanobacteria which are enriched in ^{13}C due to HCO_3^- assimilation. The lack of a relationship between pH and $\delta^{13}C_{scum}$-$\delta^{13}C_{POC}$ may instead indicate some use of atmospheric CO_2 (Paerl and Ustach 1982), which does not vary with pH, unlike the use of HCO_3^-, which increases with pH. Relationships between pCO_2 and $\delta^{13}C_{POC}$, such as those presented here, have been used to infer paleoatmospheric CO_2 levels from the sedimentary organic $\delta^{13}C$ record (e.g., Hollander and McKenzie 1991; Freeman and Hayes 1992; Meyers 2003). Our results would complicate such an interpretation. If HCO_3^- is being actively assimilated, fractionation by RuBisCo, which is proportional to the size of the $[CO_2]_{aq}$ pool, would not be the primary control on the $\delta^{13}C_{phyto}$. We discuss the implications of our results on the use of $\delta^{13}C$ as a geologic proxy in a later section.

Both $\varepsilon_{p\text{-}POC}$ and $\varepsilon_{p\text{-}model}$ were positively correlated with pCO_2, suggesting that phytoplankton discriminated against ^{13}C more when pCO_2 was high, and assimilated more ^{13}C when pCO_2 was low (Figs. 7, 9b). Previous studies have suggested a threshold concentration of CO_2; below which CCMs are activated, active uptake of HCO_3^- is enhanced, and ε_p begins to decrease. This threshold has been suggested to exist at approximately 10–25 μM for $[CO_2]_{(aq)}$ (Hinga et al. 1994; Smyntek et al. 2012), and 393 ppm for pCO_2 (Morales-Williams et al. 2017). We identify a similar threshold, where $\delta^{13}C$ increases and ε_p rapidly decreases as pCO_2 falls below equilibrium with the atmosphere ($\sim$ 400 μatm, Fig. 9a,b). This breakpoint is consistent with CCM initiation, which likely played some role in determining fractionation factors during the bloom. However, such a mechanistic link cannot be directly established from the relationship between pCO_2 and ε_p, as in Morales-Williams et al. (2017).

Since typical values of ε_p are $\sim$ 30‰ (Keller and Morel 1999), it is intriguing that measured $\varepsilon_{p\text{-}POC}$ never exceeded

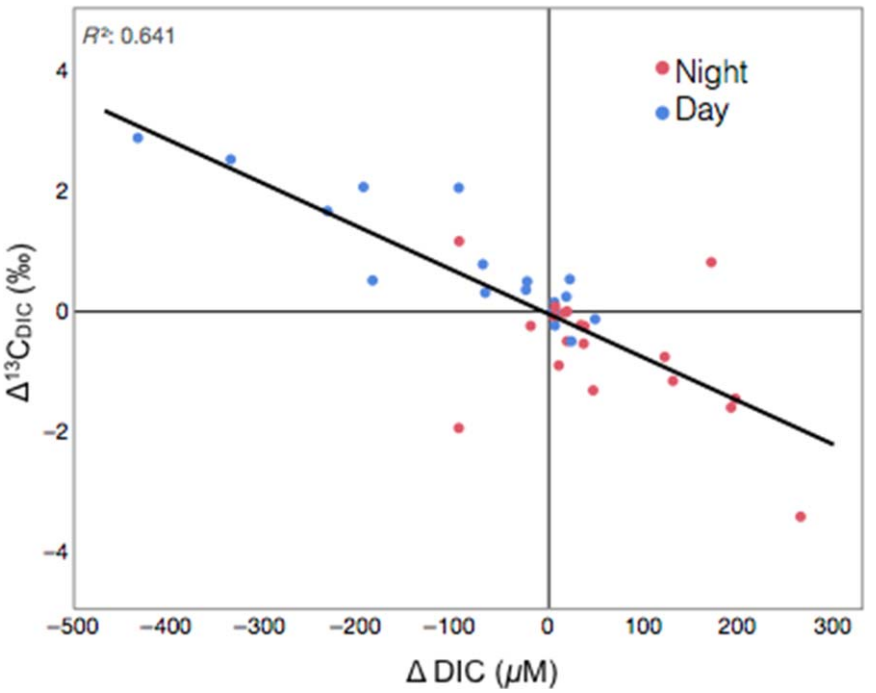

Fig. 8. Linear regression of the change in $\delta^{13}C_{DIC}$ ($\Delta^{13}C_{DIC}$; ‰) and changes in DIC (ΔDIC; μM). Changes occurring overnight are shown in red, while day-time values are shown in blue. The black line shows a linear regression with a correlation coefficient (R^2) of 0.64. [Color figure can be viewed at wileyonlinelibrary.com]

23.2‰ (Fig. 4). Despite conditions replete in DIC (865–1618 μM), rapid C uptake promoted $\delta^{13}C_{POC}$ enrichments, producing the positive relationship between $[CO_2]_{aq}$ and ε_p. A variety of factors must have contributed to this phenomenon, including: (1) growth rate (Rau et al. 1996; Keller and Morel 1999), (2) cell size and membrane permeability, (3) increased active relative to passive CO_2 uptake (Farquhar et al. 1989), (4) the fraction of C assimilated as the relatively heavy HCO_3^-, and (5) the leakage of $^{12}CO_2$ from CCMs (Kaplan and Reinhold 1999; Price et al. 2008; Hopkinson et al. 2011).

While the final factor cannot be assessed with our model, the relative importance of the remaining factors was assessed using a sensitivity test, where each parameter was allowed to vary while all others were held constant. The absolute value (in ‰) of the range in $\delta^{13}C_{phyto}$ obtained when each parameter was allowed to vary over the indicated range (Table 2) was considered to be the model sensitivity to that parameter. Rau et al. (1996, 1997) used a similar approach, and found that $\delta^{13}C_{phyto}$ was most sensitive to phytoplankton growth rate and temperature. Instead, we found that the variables ε_f and F_{HCO3} exhibited the strongest leverage on modeled $\delta^{13}C_{phyto}$ (Fig. 10). This is likely because the range in $[CO_2]_{aq}$ was large (~ 3–90 μM), including both CO_2-limiting and CO_2-replete conditions.

Physiological adaptations to CO_2 limitation are not uniform across phytoplankton taxa (Elzenga et al. 2000), and many cyanobacteria are well suited for these conditions (Paerl and Ustach 1982; Miller et al. 1990; Matsuda and Colman 1995; Shapiro 1997). Cyanobacteria and other eukaryotic algae (Tortell 2000; Reinfelder 2011) use CCMs to alleviate CO_2 limitation, allowing them to grow across a wide range of CO_2 concentrations (Badger and Spalding 2000). Many cyanobacteria can continue to grow when provided with HCO_3^- as a sole inorganic C source, although their growth rates may be decreased by 20–65% (Verspagen et al. 2014), and much of the CO_2 stored in CCMs may be lost through leakage (Kaplan and Reinhold 1999; Price et al. 2008; Hopkinson et al. 2011; Eichner et al. 2015). A variety of strategies constitute these CCMs, including active CO_2 and HCO_3^- transporters, carboxysomes in which low O_2 : CO_2 ratios may be maintained, and the production of extracellular carbonic anhydrase (Kaplan and Reinhold 1999; Price et al. 2008). In particular, *Microcystis aeruginosa* copes with variable pCO_2 by upregulating CCM genes over hourly (Jensen et al. 2011; Sandrini et al. 2016), and longer time scales (Sandrini et al. 2016). *Microcystis* expresses the greatest affinity for DIC at relatively high temperatures (20–35°C; Wu et al. 2011), indicating that the prevalence of *Microcystis* during the summer (Takahashi 1990; Wu et al. 2006; Paerl and Huisman 2008; Qin et al. 2010) may be due to their unique ability to utilize inorganic C.

In the present study, taxonomic dominance by cyanobacteria was significantly negatively correlated with pCO_2

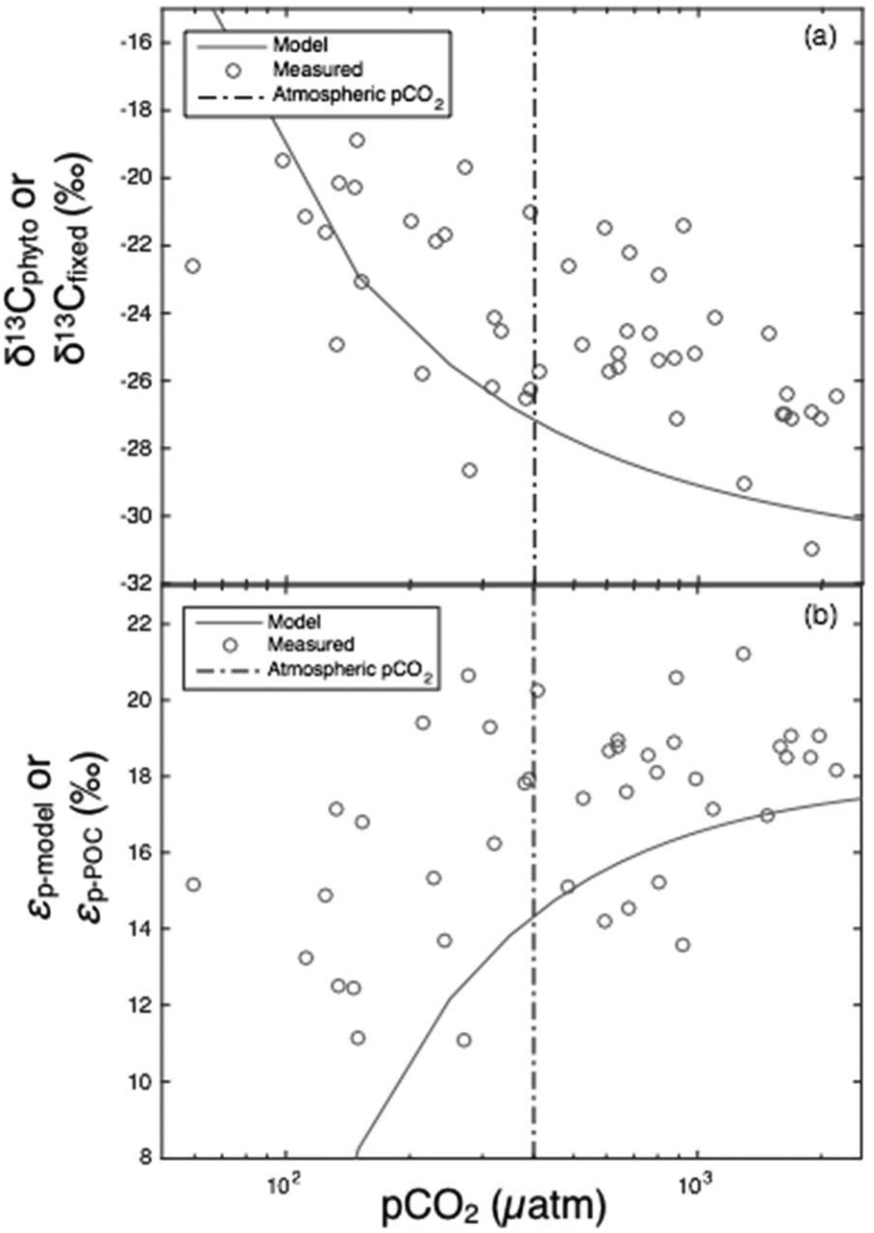

Fig. 9. Calculated $\delta^{13}C_{fixed}$ and modeled $\delta^{13}C_{phyto}$ (‰) as a function of pCO_2 (μatm)(**a**). Measured and modeled fractionation factors ($\varepsilon_{p\text{-}POC}$ and $\varepsilon_{p\text{-}model}$, respectively [‰]) vs. pCO_2 (μatm) (**b**). In both figures, the vertical black line represents approximate equilibrium between pCO_2 and atmospheric CO_2 ($\sim$ 400 μatm).

(Fig. 6), and accompanied by decreased ε_p, as well as an isotopic enrichment in $\delta^{13}C_{Fixed}$. We suggest that when N and P are replete, as they were during this study, cyanobacteria dominate due to their physiological adaptations to CO_2-limited conditions.

Drivers of $\delta^{13}C_{DIC}$

Biological consumption and production of DIC over consecutive diel cycles, caused a DIC drawdown of $\sim$ 300 μM over the study period (Fig. 3). Diel DIC excursions were further quantified as the change in DIC between dawn and dusk samples (ΔDIC), where by convention, positive values indicate net production of DIC. Diel $\delta^{13}C_{DIC}$ excursions were similarly quantified as $\Delta^{13}C_{DIC}$, where positive values indicate an isotopic enrichment of ^{13}C in DIC. As seen in Fig. 8, $\Delta^{13}C_{DIC}$ was variable, ranging from -3.4‰ to 2.9‰, with an average excursion of approximately 0.9‰. Both $\Delta^{13}C_{DIC}$ and ΔDIC were strongly negatively correlated with each other ($R^2 = 0.64$), suggesting that day-time productivity drove isotopic enrichment of $\delta^{13}C_{DIC}$, while night-time respiration

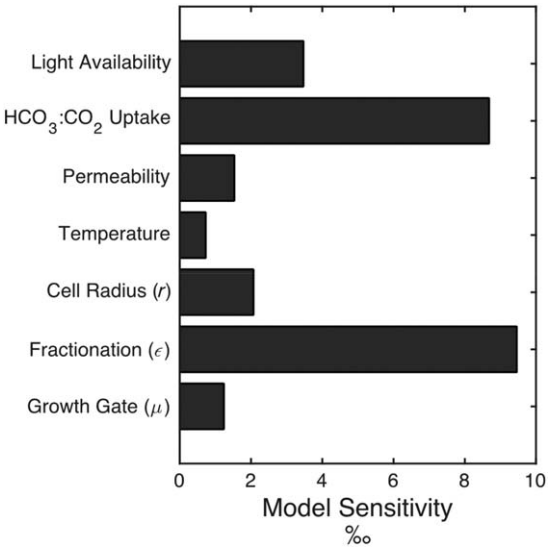

Fig. 10. Sensitivity analysis of model variables, shown as the range in $\delta^{13}C_{phyto}$ (‰) between maximum and minimum parameter values.

returned ^{12}DIC to the water column, decreasing $\delta^{13}C_{DIC}$. It is likely that patterns of hystereresis would obscure these linear trends between $\Delta^{13}C_{DIC}$ and ΔDIC if data were collected over shorter time intervals (Tobias and Böhlke 2011).

The assimilation of $CO_{2(aq)}$ shifts the carbonate equilibrium toward CO_3^{2-}, and increases the saturation state for carbonate minerals, including calcite ($CaCO_3$). Calcite saturation state ($\Omega_{Calcite}$) is defined as $\Omega_{Calcite} = (\alpha_{Ca} * \alpha_{CO3})/K_{sp}$, where α is the activity of Ca^{2+} or CO_3^{2-}, and K_{sp} is the temperature dependent solubility product for calcite. Calcite precipitation is favorable when $\Omega_{Calcite}$ is greater than 1. Lake "Whiting events" occur when biologically-driven increases in Ω cause rapid calcite precipitation, giving water a cloudy appearance, and are frequent in eutrophic lakes (Hodell et al. 1998). In this study, high pH caused high $\Omega_{Calcite}$, exceeding10 for long periods of time (Supporting Information Fig. S2). If calcite is assumed to rapidly precipitate when $\Omega_{Calcite} > 10$, then this process should have been a factor for ~ 50% of the study period. However, calcite particles were never observed in lake water or filtered solids, and could not be identified by x-ray diffraction (Holbach pers. comm.). Furthermore, acid fumingation had no effect on $\delta^{13}C_{POC}$, and $[Ca^{2+}]$ was stable and not significantly correlated with $\delta^{13}C_{DIC}$ ($R^2 = 0.003$), suggesting that rates of carbonate precipitation were small, relative to other biological processes.

The process of methanogenesis exerts a large fractionation factor, producing isotopically light CH_4, and heavy DIC (Botz et al. 1996). Because CH_4 is sparingly soluble, most of this light CH_4 can be released to the atmosphere through ebbulition or diffusive exchange before it can be oxidized to CO_2 (Bastviken et al. 2008). Large enrichments in $\delta^{13}C_{DIC}$ were attributed to this process in Lake Apopka, a shallow, hypereutrophic system similar to Taihu (Gu et al. 2004). While dissolved CH_4 was always above equilibrium with the atmosphere in Taihu (Fig. 3), no significant relationship was observed between CH_4 and $\delta^{13}C_{DIC}$ ($p = 0.81$, $r^2 < 0.001$). Hence, it is unlikely that methanogenesis was an important factor in any observed $\delta^{13}C_{DIC}$ enrichments.

To summarize, any change in $\delta^{13}C_{DIC}$ present on the weekly time scale, due to the DIC consumption and dilution, was swamped by variability over the diel time scale (Fig. 8). While factors like methanogenesis and air–water CO_2 exchange may have been important at times (Fig. 2), $\delta^{13}C_{DIC}$ was most sensitive to processes acting on the diel time scale that consume and produce DIC, namely photoautotrophic production and respiration.

δ^{13}C as a paleoclimate indicator

$\delta^{13}C_{POC}$ has long been used as an indicator of paleoatmospheric pCO_2 (Hollander and Mckenzie 1991; Meyers 2003). Hollander and McKenzie (1991) show a log-linear relationship between epilimnic $[CO_2]_{aq}$ and $\Delta^{13}C$, and suggest that it was driven primarily by the co-variation of ε_p with $[CO_2]_{aq}$, and by the ecological shift toward HCO_3^- utilizing cyanobacteria at low $[CO_2]_{aq}$. This relationship was then applied to sediment core derived estimates of ε_p in order to model $[CO_2]_{aq}$ and atmospheric pCO_2 in the geologic past. These studies have relied on samples collected at weekly or monthly intervals. An implicit assumption is that epilimnic $[CO_2]_{aq}$ and $\delta^{13}C_{POC}$ at the time of measurement are representative of that recorded in the geologic record, which may not always be the case (Ziegler and Fogel 2003; Xu et al. 2008). Xu et al. (2008) attributed an increased $\delta^{13}C_{POC}$ during the day to substrate limitation, while Ziegler and Fogel (2003) suggested shifts between phytoplankton and bacterial production drove diel fluctuations in $\delta^{13}C_{POC}$. In this study, we show large fluctuations in epilimnic $\delta^{13}C_{POC}$ over consecutive diel cycles for a full month. If relationships between $\delta^{13}C_{POC}$ and $[CO_2]_{aq}$ are to be established in surface waters, then extended to the sediments as a paleoatmospheric tool, variations on the diel scale should be acknowledged and accounted for if possible. Furthermore, it may be that C acquisition by cyanobacteria may be more sensitive to pH, rather than CO_2 availability (Mangan et al. 2016; Wang et al. 2016), an argument that is supported by the fact that modeled ε_p was most sensitive to F_{HCO3}, which is a function of pH. Care should thus be taken when interpreting sedimentary $\delta^{13}C_{POC}$ in the context of atmospheric CO_2.

Conclusion

In this study, we investigated the variability and environmental controls on stable C isotopes and algal taxonomy over diel to weekly time scales in the hypereutrophic Lake Taihu, China. We hypothesized that CO_2 limitation would be associated with the taxonomic dominance of HAB-forming cyanobacteria, and used both modeled data and

direct measurements to probe this hypothesis. The strong negative correlation between cyanobacterial relative abundance and pCO_2, as well as the positive relationship between pCO_2 and isotope fractionation factors (ε_p) supports our hypothesis. Furthermore, that modeled $\delta^{13}C_{phyto}$ was most sensitive to changes in carbon acquisition (F_{HCO3}, ε_f), as opposed to factors like growth rate and temperature, supported the role of CO_2 limitation in bloom dynamics. Specific factors related to carbon acquisition, namely CO_2 leakage from CCMs, were not assessed during this study, but are clearly important factors in cellular isotope budgets. Future studies investigating rates and consequences of CO_2 leakage are warranted. Despite high pH and dissolved CH_4, authigenic calcite precipitation and methanogenesis were not significant parts of the isotope budget. Instead, net ecosystem production and respiration caused $\delta^{13}C_{DIC}$ to vary over consecutive diel cycles. We suggest that the ability of cyanobacteria to cope with CO_2 limitation is an important factor promoting their dominance during bloom events. As HABs are expected to increase in frequency and severity with rising CO_2 levels, our understanding of C cycling during these events will help us predict how HABs will respond to a changing climate.

References

Abril, G., and others. 2015. Technical note: Large overestimation of pCO_2 calculated from pH and alkalinity in acidic, organic-rich freshwaters. Biogeosciences **12**: 67–78. doi:10.5194/bg-12-67-2015

Aizawa, K., and S. Miyachi. 1986. Carbonic anhydrase and CO_2 concentrating mechanisms in microalgae and cyanobacteria. FEMS Microbiol. Lett. **39**: 215–233. doi:10.1016/0378-1097(86)90447-7

Anderson, D. M., P. M. Glibert, and J. M. Burkholder. 2002. Harmful algal blooms and eutrophication: Nutrient sources, composition, and consequences. Estuaries **25**: 704–726. doi:10.1007/BF02804901

Badger, M. R., and M. H. Spalding. 2000. CO_2 acquisition, concentration and fixation in cyanobacteria and algae, p. 369–397. *In* R. C. Leegood, T. D. Sharkey, and S. von Caemmerer [eds.], Photosynthesis: Physiology and metabolism. Kluwer Academic Publishers.

Bastviken, D., J. J. Cole, M. L. Pace, and M. C. Van de-Bogert. 2008. Fates of methane from different lake habitats: Connecting whole-lake budgets and CH_4 emissions. J. Geophys. Res. Biogeosci. **113**: G02024. doi:10.1029/2007JG000608

Battin, T. J., S. Luyssaert, L. A. Kaplan, A. K. Aufdenkampe, A. Richter, and L. J. Tranvik. 2009. The boundless carbon cycle. Nat. Geosci. **2**: 598–600. doi:10.1038/ngeo618

Botz, R., H. D. Pokojski, M. Schmitt, and M. Thomm. 1996. Carbon isotope fractionation during bacterial methanogenesis by CO_2 reduction. Org. Geochem. **25**: 255–262. doi:10.1016/S0146-6380(96)00129-5

Burkhardt, S., U. Riebesell, and I. Zondervan. 1999. Effects of growth rate, CO_2 concentration, and cell size on the stable carbon isotope fractionation in marine phytoplankton. Geochim. Cosmochim. Acta **63**: 3729–3741. doi:10.1016/S0016-7037(99)00217-3

Cai, W.-J., and Y. Wang. 1998. The chemistry, fluxes, and sources of carbon dioxide in the estuarine waters of the Satilla and Altamaha Rivers, Georgia. Limnol. Oceanogr. **43**: 657–668. doi:10.4319/lo.1998.43.4.0657

de Kluijver, A., J. Yu, M. Houtekamer, J. J. Middelburg, and Z. Liu. 2012. Cyanobacteria as a carbon source for zooplankton in eutrophic Lake Taihu, China, measured by ^{13}C labeling and fatty acid biomarkers. Limnol. Oceanogr. **57**: 1245–1254. doi:10.4319/lo.2012.57.4.1245

Eby, P., J. J. Gibson, and Y. Yi. 2015. Suitability of selected free-gas and dissolved-gas sampling containers for carbon isotopic analysis. Rapid Commun. Mass Spectrom. **29**: 1215–1226. doi:10.1002/rcm.7213

Eichner, M., S. Thoms, S. A. Kranz, and B. Rost. 2015. Cellular inorganic carbon fluxes in Trichodesmium: A combined approach using measurements and modelling. J. Exp. Bot. **66**: 749–759. doi:10.1093/jxb/eru427

Elzenga, J. T. M., H. B. A. Prins, and J. Stefels. 2000. The role of extracellular carbonic anhydrase activity in inorganic carbon utilization of *Phaeocystis globosa* (Prymnesiophyceae): A comparison with other marine algae using the isotopic disequilibrium technique. Limnol. Oceanogr. **45**: 372–380. doi:10.4319/lo.2000.45.2.0372

Farquhar, G., J. Ehleringer, and K. Hubick. 1989. Carbon isotope discrimination and photosynthesis. Annu. Rev. Plant Physiol. **40**: 503–537. doi:10.1146/annurev.pp.40.060189.002443

Freeman, K. H., and J. M. Hayes. 1992. Fractionation of carbon isotopes by phytoplankton and estimates of ancient CO_2 levels. Global Biogeochem. Cycles **6**: 185–198. doi:10.1029/92GB00190

Gu, B., and V. Alexander. 1997. Stable carbon isotope evidence for atmospheric CO_2 uptake by cyanobacterial surface scums. Appl. Environ. Microbiol. **62**: 1803–1804.

Gu, B., C. L. Schelske, and D. A. Hodell. 2004. Extreme ^{13}C enrichments in a shallow hypereutrophic lake: Implications for carbon cycling. Limnol. Oceanogr. **49**: 1152–1159. doi:10.4319/lo.2004.49.4.1152

Gu, B., A. D. Chapman, and C. L. Schelske. 2006. Factors controlling seasonal variations in stable isotope composition of particulate organic matter in a softwater eutrophic lake. Limnol. Oceanogr. **51**: 2837–2848. doi:10.4319/lo.2006.51.6.2837

Gu, B., C. L. Schelske, and M. N. Waters. 2011. Patterns and controls of seasonal variability of carbon stable isotopes of particulate organic matter in lakes. Oecologia **165**: 1083–1094. doi:10.1007/s00442-010-1888-6

Hinga, K. R., M. A. Arthur, M. E. Q. Pilson, and D. Whitaker. 1994. Carbon isotope fractionation by marine phytoplankton in culture: The effects of CO2 concentration,

pH, temperature, and species. Glob. Biochem. Cycles **8**: 91–102.

Hinners, J., R. Hofmeister, and I. Hense. 2015. Modeling the role of pH on Baltic Sea cyanobacteria. Life **5**: 1204–1217. doi:10.3390/life5021204

Hodell, D. A., C. L. Schelske, G. L. Fahnenstiel, and L. L. Robbins. 1998. Biologically induced calcite and its isotopic composition in Lake Ontario. Limnol. Oceanogr. **43**: 187–199. doi:10.4319/lo.1998.43.2.0187

Hollander, D. J., and J. A. McKenzie. 1991. CO_2 control on carbon-isotope fractionation during aqueous photosynthesis: A paleo-pCO_2 barometer. Geology **19**: 929–932. doi:10.1130/0091-7613(1991)019<0929:CCOCIF>2.3.CO;2

Hopkinson, B. M. 2014. A chloroplast pump model for the CO_2 concentrating mechanism in the diatom *Phaeodactylum tricornutum*. Photosynth. Res. **121**: 223–233. doi:10.1007/s11120-013-9954-7

Hopkinson, B. M., C. L. Dupontb, A. E. Allenb, and F. M. M. Morela. 2011. Efficiency of the CO_2-concentrating mechanism of diatoms. Proc. Natl. Acad. Sci. USA **108**: 3830–3837. doi:10.1073/pnas.1018062108

Hopkinson, B. M., C. L. Dupont, and Y. Matsuda. 2016. The physiology and genetics of CO_2 concentrating mechanisms in model diatoms. Curr. Opin. Plant Biol. **31**: 51–57. doi:10.1016/j.pbi.2016.03.013

Jensen, S. I., A.-S. Steunou, D. Bhaya, M. Kühl, and A. R. Grossman. 2011. In situ dynamics of O_2, pH and cyanobacterial transcripts associated with CCM, photosynthesis and detoxification of ROS. ISME J. **5**: 317–328. doi:10.1038/ismej.2010.131

Kaplan, A., and L. Reinhold. 1999. CO_2 concentrating mechanisms in photosynthetic microorganisms. Annu. Rev. Plant Physiol. **50**: 539–570. doi:10.1146/annurev.arplant.50.1.539

Keller, K., and F. M. M. Morel. 1999. A model of carbon isotopic fractionation and active carbon uptake in phytoplankton. Mar. Ecol. Prog. Ser. **182**: 295–298. doi:10.3354/meps182295

Lammers, J. M., G. J. Reichart, and J. J. Middelburg. 2017. Seasonal variability in phytoplankton stable carbon isotope ratios and bacterial carbon sources in a shallow Dutch lake. Limnol. Oceanogr. **62**: 2773–2787. doi:10.1002/lno.10605

Lewitus, A. J., D. L. White, R. G. Tymowski, M. E. Geesey, S. N. Hymel, and P. A. Noble. 2005. Adapting the CHEMTAX method for assessing phytoplankton taxonomic composition in southeastern U.S. estuaries. Estuaries **28**: 160–172. doi:10.1007/BF02732761

Li, S., J. Zhou, L. Wei, F. Kong, and X. Shi. 2016. The effect of elevated CO_2 on autotrophic picoplankton abundance and production in a eutrophic lake (Lake Taihu, China). Mar. Freshw. Res. **67**: 319–326. doi:10.1071/MF14353

Liu, X., X. Lu, and Y. Chen. 2011. The effects of temperature and nutrient ratios on *Microcystis* blooms in Lake Taihu, China: An 11-year investigation. Harmful Algae **10**: 337–343. doi:10.1016/j.hal.2010.12.002

Lu, Y., P. A. Meyers, B. J. Eadie, and J. A. Robbins. 2010. Carbon cycling in Lake Erie during cultural eutrophication over the last century inferred from the stable carbon isotope composition of sediments. J. Paleolimnol. **43**: 261–272. doi:10.1007/s10933-009-9330-y

Maberly, S. C., P. A. Barker, A. W. Stott, D. Ville, and M. Mitzi. 2013. Catchment productivity controls CO_2 emissions from lakes. Nat. Clim. Chang. **3**: 391–394. doi:10.1038/nclimate1748

Mackey, M. D., D. J. Mackey, H. W. Higgins, and S. W. Wright. 1996. CHEMTAX - a program for estimating class abundances from chemical markers: Application to HPLC measurements of phytoplankton. Mar. Ecol. Prog. Ser. **144**: 265–283. doi:10.3354/meps144265

Mangan, N. M., A. Flamholz, R. D. Hood, R. Milo, and D. F. Savage. 2016. pH determines the energetic efficiency of the cyanobacterial CO_2 concentrating mechanism. Proc. Natl. Acad. Sci. USA **113**: E5354–E5362. doi:10.1073/pnas.1525145113

Marotta, H., L. Pinho, C. Gudasz, D. Bastviken, L. J. Tranvik, and A. Enrich-Prast. 2014. Greenhouse gas production in low-latitude lake sediments responds strongly to warming. Nat. Clim. Chang. **4**: 467–414. doi:10.1038/nclimate2222

Matsuda, Y., and B. Colman. 1995. Induction of CO_2, and bicarbonate transport in the green alga chlorella ellipsoidea. Plant Physiol. **108**: 253–260. doi:10.1104/pp.108.1.253

McQueen, D. J., and D. R. S. Lean. 1987. Influence of water temperature and nitrogen to phosphorus fatios on the dominance of blue-green algae in Lake St. George, Ontario. Can. J. Fish. Aquat. Sci. **44**: 598–604. doi:10.1139/f87-073

Meyers, P. A. 2003. Application of organic geochemistry to paleolimnological reconstruction: A summary of examples from the Laurention Great Lakes. Org. Geochem. **34**: 261–289. doi:10.1016/S0146-6380(02)00168-7

Miller, J. D., G. S. Espie, and D. T. Canvin. 1990. Physiological aspects of CO_2 and HCO_3 transport by cyanobacreria: A review. Can. J. Bot. **68**: 1291–1302. doi:10.1139/b90-165

Mook, W., J. Bommerson, and W. Staverman. 1974. Carbon isotope fractionation between dissolved bicarbonate and gaseous carbon dioxide. Earth Planet. Sci. Lett. **22**: 169–176. doi:10.1016/0012-821X(74)90078-8

Morales-Williams, A. M., A. D. Wanamaker, and J. A. Downing. 2017. Cyanobacterial carbon concentrating mechanisms facilitate sustained CO_2 depletion in eutrophic lakes. Biogeosciences **14**: 2865–2875. doi:10.5194/bg-14-2865-2017

O'Leary, M. H. 1984. Measurement of the isotope fractionation associated with diffusion of carbon dioxide in aqueous solution. J. Phys. Chem. **88**: 823–825. doi:10.1021/j150648a041

Otten, T. G., H. Xu, B. Qin, G. Zhu, and H. W. Paerl. 2012. Spatiotemporal patterns and ecophysiology of toxigenic *Microcystis* blooms in Lake Taihu, China: Implications for water quality management. Environ. Sci. Technol. **46**: 3480–3488. doi: 10.1021/es2041288

Pacheco, F. S., F. Roland, and J. A. Downing. 2014. Eutrophication reverses whole-lake carbon budgets. Inland Waters **4**: 41–48. doi:10.5268/IW-4.1.614

Paerl, H. W. 1983. Partitioning of CO_2 fixation in the colonial cyanobacterium *Microcystis aeruginosa*: Mechanism promoting formation of surface scums. Appl. Environ. Microbiol. **46**: 252–259.

Paerl, H. W., and J. Ustach. 1982. Blue-green algal scums: An explanation for their occurrence during freshwater blooms. Limnol. Oceanogr. **27**: 212–217. doi:10.4319/lo.1982.27.2.0212

Paerl, H. W., and J. Huisman. 2008. Blooms like it hot. Science **320**: 57–58. doi:10.1126/science.1155398

Paerl, H. W., and J. Huisman. 2009. Climate change: A catalyst for global expansion of harmful cyanobacterial blooms. Environ. Microbiol. Rep. **1**: 27–37. doi:10.1111/j.1758-2229.2008.00004.x

Paerl, H. W., H. Xu, M. J. McCarthy, G. Zhu, B. Qin, Y. Li, and W. S. Gardner. 2011. Controlling harmful cyanobacterial blooms in a hyper-eutrophic lake (Lake Taihu, China): The need for a dual nutrient (N & P) management strategy. Water Res. **45**: 1973–1983. doi:10.1016/j.watres.2010.09.018

Paerl, H. W., and others. 2014. Controlling cyanobacterial blooms in hypertrophic Lake Taihu, China: Will nitrogen reductions cause replacement of non-N_2 fixing by N_2 fixing taxa? PLoS One **9**: e113123. doi:10.1371/journal.pone.0113123

Paerl, H. W., H. Xu, N. S. Hall, K. L. Rossignol, A. R. Joyner, G. Zhu, and B. Qin. 2015. Nutrient limitation dynamics examined on a multi-annual scale in Lake Taihu, China: Implications for controlling eutrophication and harmful algal blooms. J. Freshw. Ecol. **30**: 5–24. doi:10.1080/02705060.2014.994047

Pinckney, J. L., T. L. Richardson, D. F. Millie, and H. W. Paerl. 2001. Application of photopigment biomarkers for quantifying microalgal community composition and in situ growth rates. Org. Geochem. **32**: 585–595. doi:10.1016/S0146-6380(00)00196-0

Popp, B. N., E. A. Laws, R. R. Bridigare, J. E. Dore, K. L. Hanson, and S. G. Wakeham. 1998. Effect of phytplankton cell geometry on carbon isotope fractionation. Geochim. Cosmochim. Acta **62**: 69–77. doi:10.1016/S0016-7037(97)00333-5

Price, G. D. 2011. Inorganic carbon transporters of the cyanobacterial CO2 concentrating mechanism. Photosynth. Res. **109**: 47–57. doi:10.1007/s11120-010-9608-y

Price, G. D., M. R. Badger, F. J. Woodger, and B. M. Long. 2008. Advances in understanding the cyanobacterial CO_2-concentrating- mechanism (CCM): Functional components, C_i transporters, diversity, genetic regulation and prospects for engineering into plants. J. Exp. Bot. **59**: 1441–1461. doi:10.1093/jxb/erm112

Qin, B., G. Zhu, G. Gao, Y. Zhang, W. Li, H. W. Paerl, and W. W. Carmichael. 2010. A drinking water crisis in Lake Taihu, China: Linkage to climatic variability and lake management. Environ. Manag. **45**: 105–112. doi:10.1007/s00267-009-9393-6

Rau, G. H., U. Riebesell, and D. Wolf-Gladrow. 1996. A model of photosynthetic ^{13}C fractionation by marine phytoplankton based on diffusive molecular CO_2 uptake. Mar. Ecol. Prog. Ser. **133**: 275–285. doi:10.3354/meps133275

Rau, G. H., D. Wolf-Gladrow, and U. Riebesell. 1997. CO_{2aq}-dependent photosynthetic ^{13}C fractionation in the ocean: A model versus measurements. Global Biogeochem. Cycles **11**: 267–278. doi:10.1029/97GB00328

Reinfelder, J. R. 2011. Carbon concentrating mechanisms in eukaryotic marine phytoplankton. Ann. Rev. Mar. Sci. **3**: 291–315. doi:10.1146/annurev-marine-120709-142720

Sandrini, G., R. P. Tann, J. M. Schuurmans, S. A. M. van Beusekom, H. C. P. Matthijs, and J. Huisman. 2016. Diel variation in gene expression of the CO_2-concentrating mechanism during a harmful cyanobacterial bloom. Front. Microbiol. **7**: 1–16. doi:10.3389/fmicb.2016.00551

Schlüter, L., T. L. Lauridsen, G. Krogh, and T. Jørgensen. 2006. Identification and quantification of phytoplankton groups in lakes using new pigment ratios - a comparison between pigment analysis by HPLC and microscopy. Freshw. Biol. **51**: 1474–1485. doi:10.1111/j.1365-2427.2006.01582.x

Shapiro, J. 1997. The role of carbon dioxide in the initiation and maintenance of blue-green dominance in lakes. Freshw. Biol. **37**: 307–323. doi:10.1046/j.1365-2427.1997.00164.x

Shi, K., Y. Zhang, H. Xu, and others. 2015. Long-Term Satellite Observations of Microcystin Concentrations in Lake Taihu during Cyanobacterial Bloom Periods. Environ. Sci. Technol. **49**: 6448–6456. doi:10.1021/es505901a

Smyntek, P. M., S. C. Maberly, and J. Grey. 2012. Dissolved carbon dioxide concentration controls baseline stable carbon isotope signatures of a lake food web. Limnol. Oceanogr. **57**: 1292–1302. doi:10.4319/lo.2012.57.5.1292

Takahashi, K. 1990. Temporal variations in carbon isotope ratio of phytoplankton in a eutrophic lake. J. Plankton Res. **12**: 799–808. doi:10.1093/plankt/12.4.799

Tobias, C., and J. K. Böhlke. 2011. Biological and geochemical controls on diel dissolved inorganic carbon cycling in a low-order agricultural stream: Implications for reach scales and beyond. Chem. Geol. **283**: 18–30. doi:10.1016/j.chemgeo.2010.12.012

Toming, K., and others. 2013. Contributions of autochthonous and allochthonous sources to dissolved organic matter in a large, shallow, eutrophic lake with a highly calcareous catchment. Limnol. Oceanogr. **58**: 1259–1270. doi:10.4319/lo.2013.58.4.1259

Tortell, P. D. 2000. Evolutionary and ecological perspectives on carbon acquisition in phytoplankton. Limnol. Oceanogr. **45**: 744–750. doi:10.4319/lo.2000.45.3.0744

Tranvik, L. J., and others. 2009. Lakes and reservoirs as regulators of carbon cycling and climate. Limnol. Oceanogr. **54**: 2298–2314. doi:10.4319/lo.2009.54.6_part_2.2298

Van Heukelem, L., A. Lewitus, T. Kana, and N. Craft. 1994. Improved separations of phytoplankton pigments using temperature-controlled high performance liquid chromatography. Mar. Ecol. Prog. Ser. **114**: 303–313. doi:10.3354/meps114303

Verspagen, J. M. H., D. B. Van de Waal, J. F. Finke, P. M. Visser, E. Van Donk, and J. Huisman. 2014. Rising CO_2 levels sill intensify phytoplankton blooms in eutrophic and hypertrophic lakes. PLoS One **9**: e104325. doi:10.1371/journal.pone.0104325

Wang, S., K. M. Yeager, and W. Lu. 2016. Carbon isotope fractionation in phytoplankton as a potential proxy for pH rather than for $[CO_{2(aq)}]$: Observations from a carbonate lake. Limnol. Oceanogr. **61**: 1259–1270. doi:10.1002/lno.10289

Wanninkhof, R. 1992. Relationship between wind speed and gas exchange. J. Geophys. Res. **97**: 7373–7382. doi:10.1029/92JC00188

Wu, S. K., P. Xie, G. D. Liang, S. B. Wang, and X. M. Liang. 2006. Relationships between microcystins and environmental parameters in 30 subtropical shallow lakes along the Yangtze River, China. Freshw. Biol. **51**: 2309–2319. doi:10.1111/j.1365-2427.2006.01652.x

Wu, X., Z. Wu, and L. Song. 2011. Phenotype and temperature affect the affinity for dissolved inorganic carbon in a cyanobacterium Microcystis. Hydrobiologia **675**: 175–186. doi:10.1007/s10750-011-0815-0

Xu, H., H. W. Paerl, B. Qin, G. Zhu, and G. Gao. 2010. Nitrogen and phosphorus inputs control phytoplankton growth in eutrophic Lake Taihu, China. Limnol. Oceanogr. **55**: 420–432. doi:10.4319/lo.2010.55.1.0420

Xu, J., M. Zhang, and P. Xie. 2007. Stable carbon isotope variations in surface bloom scum and subsurface seston among shallow eutrophic lakes. Harmful Algae **6**: 679–685. doi:10.1016/j.hal.2007.02.002

Xu, J., P. Xie, and J. Qin. 2008. Diel isotopic fluctuation in surface seston and its physiological. **44**: 197–201. doi:10.1051/limn:2008004

Yoon, T. K., H. Jin, N. H. Oh, and J. H. Park. 2016. Technical note: Assessing gas equilibration systems for continuous pCO_2 measurements in inland waters. Biogeosciences **13**: 3915–3930. doi:10.5194/bg-13-3915-2016

Yu, L., F. Kong, X. Shi, Z. Yang, M. Zhang, and Y. Yu. 2014. Effects of elevated CO_2 on dynamics of microcystin-producing and non-microcystin-producing strains during *Microcystis* blooms. J. Environ. Sci. **27**: 251–258. doi:10.1016/j.jes.2014.05.047

Ziegler, S. E., and M. L. Fogel. 2003. Seasonal and diel relationships between the isotopic compositions of dissolved and particulate organic matter in freshwater ecosystems. Ecosystems **64**: 25–52. doi:10.1023/A:1024989915550

Acknowledgments

Andre Wilhelms provided assiastance in the field, and Marina Doeringer helped with analytical work. We thank Guangwei Zhu for providing meterological and hydrographic data. We also thank Marc Alperin for the meticulous and illuminating discussions, as well as Wenqing Shi for his helpful comments. The authors are grateful for the support of the Chinese Ministry of Science and Technology (2015DFG91980), as well as the staff at the Taihu Laboratory for Lake Ecosystem Research (TLLER). We stress that the science and international collaborations stemming from this project would have been impossible without assistance from National Science Foundation's East Asia and Pacific Summer Institutes program (EAPSI fellowship: 1614132). Trans-national initiatives such as EAPSI acquaint young scientists with science infrastructure, policy, and cultures around the world, and allow them to establish the international co-operations that are critical to solving today's problems. Continued funding for these programs ensures that future generations are not excluded from the global scientific community. Technical support was provided by Randy Sloup and Karen Rossignol at the UNC Institute of Marine Sciences. This research was also supported by a Federal Ministry of Education and Research of Germany (BMBF grant 02WCL1336B), and the US National Science Foundation (CBET 1230543 and Dimensions of Biodiversity 1240851).

Conflict of Interest

None declared.

Submitted 18 November 2017
Revised 22 January 2018
Accepted 12 February 2018

Associate editor: Maren Voss